THE JOURNAL OF PHYSICAL CHEMISTRY B
A JOURNAL OF THE AMERICAN CHEMICAL SOCIETY

pubs.acs.org/JPCB

Article

Real Electrolyte Solutions in the Functionalized Mean Spherical Approximation: A Density Functional Theory for Simple Electrolyte Solutions

Elvis do A. Soares,* Nathalia S. Vernin, Mirella S. Santos, and Frederico W. Tavares*

Cite This: https://doi.org/10.1021/acs.jpcb.2c00816

Read Online

ACCESS | Metrics & More | Article Recommendations | Supporting Information

ABSTRACT: The equation of state based on the mean spherical approximation (MSA) can describe electrolyte solutions as a primitive model, where the ions are charged hard-sphere particles and the solvent is a continuum medium. In recent years, many propositions of the classical density functional theory (cDFT) for electrolyte solutions have been presented. One of these is the functionalized MSA (fMSA) which has proven to be a great functional approach of MSA to calculate the electric double layer structures. This work demonstrates how the fMSA theory can describe real electrolyte solutions (e.g., NaCl, KI, and LiBr) where hydration and solvent concentration effects are present. Experimental data of the mean activity coefficients of different simple salts were successfully reproduced. When the hydrated diameter and the electrolyte solution electric permittivity are used, the fMSA predicts a charge inversion on the electrostatic potential near a charged surface at high salt concentrations.

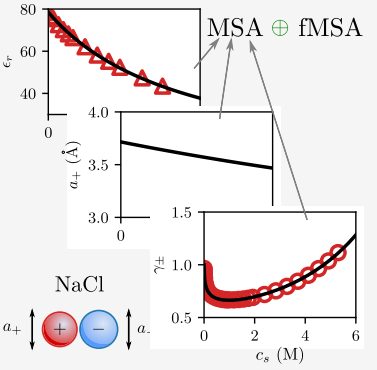

1. INTRODUCTION

Electrolyte systems and processes involving charges are ubiquitous. Over the years, many theories have been proposed to describe counterintuitive phenomena, such as charge inversion,[1,2] the attraction between like-charged surfaces,[3,4] and long-range oscillatory densities.[5] However, the description of ionic distribution profile close to interfaces[6,7] and/or colloidal macroparticles[8,9] is not always accurate despite efforts to develop suitable theories for all electrolyte solutions and conditions.

In this context, some versions of classical density functional theory (cDFT) have been proposed to describe the ion electrostatic correlation as the "old but gold" bulk fluid density approximation (BFD),[10−12] which consist of a second-order Taylor's expansion of the excess free energy around the densities at the bulk solution, the functionalized mean spherical approximation (fMSA),[13] and the reference fluid density approximation (RFD).[14,15] Both fMSA and RFD describe well the double layer structure even for divalent and trivalent ions.[7] Although RFD is the most accurate describing small ions cases, fMSA is less computationally expensive than RFD.[16]

In primitive models, the ions are represented by hard-sphere particles and the solvent by a continuum medium whose characteristics are described by the dielectric constant. Because the original mean spherical approximation (MSA)[17−20] is a primitive model, the fMSA has some issues describing real electrolyte solutions, as it cannot reproduce experimental mean activity coefficients. Usually, its performance is compared to Monte Carlo simulation data rather than experimental data.

The original version of the MSA-based equation of state cannot predict the experimental activity and osmotic coefficients of simple salt solutions (e.g., NaCl) at high salt concentrations.[21] The last versions of the MSA-based equation of state[22−24] introduced the solvent effects by parametrizing the thermodynamic properties of pure electrolytes with the use of the concentration-dependent cation hard-sphere diameter and the relative electric permittivity parameter. Here, we introduce the variation of these parameters with the salt concentration into the fMSA. The effects of these corrections are taken into account explicitly for the chemical potential and the excess free energy. Compared to the original fMSA, our theory is consistent with the MSA equation of state for real ionic solutions and the experimental data of the mean activity coefficient of simple salts.

After this introduction, which presents general aspects and the motivation of this work, Section 2 presents a brief background about the mean spherical approximation to describe ion electrostatic correlations in real electrolyte solutions. The proposed strategy is performed in Section 3 and compared to experimental mean activity coefficients. Finally, Section 4 presents the conclusions of this work.

Received: February 2, 2022
Revised: July 22, 2022

2. REAL ELECTROLYTE SOLUTIONS IN THE MSA

The thermodynamic properties of electrolytes in the primitive MSA can be derived from the Helmholtz free energy density $f = f^{id} + f^{exc}$, where f^{id} is the ideal-gas contribution and f^{exc} is the excess contribution due to the interparticle interactions. We can split the excess free energy density into two terms in the form

$$f^{exc} = f^{hs} + f^{ec} \tag{1}$$

where f^{hs} is the ionic hard-sphere contribution and f^{ec} is the electrostatic contribution from the MSA. As an example, the chemical potential for each ionic species can be obtained by the derivative

$$\mu_i = \left(\frac{\partial f}{\partial \rho_i}\right)_{T,\rho_{j\neq i}} \tag{2}$$

with respect to ρ_i, the number density of ion species i keeping fixed the temperature T and $\rho_{j\neq i}$ the number density of other species j. Besides that, the excess free energy has parameters such as the hard-sphere diameters of each ion species, a_i, and the solvent relative permittivity, ϵ_r.

Real electrolyte solutions are known for presenting hydration and concentration effects.[25] These effects can be considered by introducing the concentration dependence of the relative permittivity of the solution ϵ_r and the hard-sphere diameters of the cations a_+.[22,23,26] The ion-specific dielectric decrements can be well described by the model $\epsilon_r(c_s) = \epsilon_r^{(w)}/(1 + \sum_i \alpha_\epsilon^{(i)} x_i)$, where c_s is the salt molar concentration, x_i is the mole fraction, $\epsilon_r^{(w)} = 78.5$ is the relative permittivity of water at $T = 298$ K, and $\alpha_\epsilon^{(i)}$ is a fitted parameter for each ion i in water solvent listed in ref 27. In this work, we propose that the cation hard-sphere diameter can be described by $a_+ = a_+^P + \delta_H/(1 + \alpha_H c_s)$ where a_P is the Pauling diameter of a cation and δ_H and α_H are additional parameters to correct the cation hydrated diameter. It is worth mentioning that this correlation is better than the original linear model from ref 22 because in the high salt concentration limit $c_s \to \infty$ we obtain $a_+ \to a_+^P$, the cation diameter in the solid salt. Also, in this work, the anion diameter a_- is the Pauli diameter a_-^P.[25]

Thereat, the excess chemical potential must be corrected by the relative permittivity and the hydrated cation diameter adjustments. The excess chemical potential is given by $\mu_i^{exc} = \mu_i^{hs} + \mu_i^{ec} + \mu_i^{corr}$ where each term can be calculated from

$$\mu_i^{hs} = \frac{\partial f^{hs}}{\partial \rho_i} \tag{3}$$

$$\mu_i^{ec} = \frac{\partial f^{ec}}{\partial \rho_i} \tag{4}$$

$$\mu_i^{corr} = \frac{\partial f^{exc}}{\partial a_+}\frac{\partial a_+}{\partial \rho_i} + \frac{\partial f^{exc}}{\partial \epsilon_r}\frac{\partial \epsilon_r}{\partial \rho_i} \tag{5}$$

and we omit the parentheses for convenience. The first and second terms on the rhs of eq 5 represent the hydrated cation diameter correction and the relative permittivity correction in the excess chemical potential, respectively.

3. RESULTS AND DISCUSSION

Table 1 presents the fitted cation hydrated diameter parameters, δ_H and α_H, of the hard-sphere diameter for the MSA model for different electrolyte solutions. These two parameters were fitted from the logarithm of the mean activity coefficient calculated by $\ln \gamma_\pm = {}^1/_2(\beta\mu_+^{exc} + \beta\mu_-^{exc})$, where the excess chemical potentials are obtained by the sum of eqs 3−5. At the first-order approximation, i.e., lower salt concentration, our hydrated diameter correction is equivalent to the original one from ref 21. The differences between the two corrections become important for higher salt concentrations.

Table 1. Fitted Cation Hydration Correction of the Hard-Sphere Diameter for the MSA for Different Electrolyte Solutions

salt	$\delta_H{}^a$ (nm)	$\alpha_H{}^a$ (L/mol)
LiCl	0.365(30)	0.025(13)
LiBr	0.38(13)	0.03(6)
LiI	0.4007(6)	0.0482(5)
NaCl	0.1810(1)	0.0257(1)
NaBr	0.1945(16)	0.0326(15)
NaI	0.2239(74)	0.0858(75)
KCl	0.0571(6)	0.1705(36)
KBr	0.0747(7)	0.5603(66)
KI	0.1344(69)	2.86(16)

[a]The numbers in parentheses represent the uncertainties in the last digits.

In Figure 1, we present the comparison between the three different versions of the MSA and the experimental data of the mean activity coefficient as a function of the salt concentration for different electrolyte solutions. The dotted lines represent the results from the original version of the MSA using the original Pauli's cation diameter and the water relative permittivity. The dashed lines represent the MSA with the hydrated cation diameter a_+ and the relative permittivity ϵ_r, both concentration-dependent as in ref 22 but without the chemical potential correction. The solid lines are our results, where the hydrated cation diameter a_+ with fitted parameter from Table 1 and the electrolyte relative permittivity ϵ_r from ref 27 are both concentration-dependent, leading to the necessary chemical potential $\mu_\pm$ corrections. Without the chemical potential corrections from eq 5, the mean activity coefficient can only be described until a concentration around 1.0 M. Therefore, the excess chemical potential correction terms are extremely necessary to describe the experimental data of the mean activity coefficient for the whole salt concentration values.

In Figure 2, we present the results of density profiles for NaCl at salt concentrations of 1.0, 3.0, and 5.0 M as calculated from fMSA, as presented in the Appendix. The results presented by the dashed lines use the Pauli's ionic diameters and water dielectric constant (as in the MSA curve of Figure 1), and the data presented by the solid lines use the new cation hydrated diameter and electric permittivity values presented in this paper (as in the $\mu_\pm$ curve of Figure 1). We can see that for $c_s = 1.0$ M the density profiles are very similar for original fMSA and our model. For $c_s = 3.0$ M, the electrostatic potential profiles are quite different. But for $c_s = 5.0$ M, the double layer charge inversion amplifies when we use the new hydrated cation diameter and electric permittivity values, and a charge inversion in the electric potential profile can be observed in Figure 2. There is an increase in the electrostatic potential value at $z = a_+/2$, represented by a peak in the profiles for $c_s = 3.0$ and 5.0 M. This peak is not present in the profile for $c_s = 1.0$ M. In fact, at high concentrations, the cation diameter is

https://doi.org/10.1021/acs.jpcb.2c00816
J. Phys. Chem. B XXXX, XXX, XXX−XXX

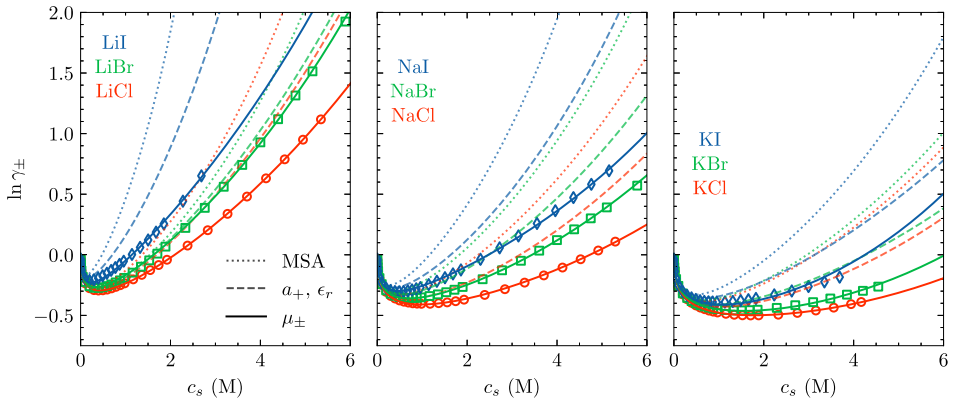

Figure 1. Logarithm of the mean activity coefficients as a function of the salt concentration at 298 K for the alkali metal halides composed by Li (left), Na (middle), and K (right). Open symbols: experimental data.[28] Dotted lines: original MSA with ionic Pauli diameters and water ϵ_r value. Dashed lines: a_+ hydrated diameter and ϵ_r, both concentration-dependent as in ref 22. Solid lines: a_+ with fitted parameter from Table 1, ϵ_r from ref 27, and the addition of the $\mu_\pm$ corrections from eq 5.

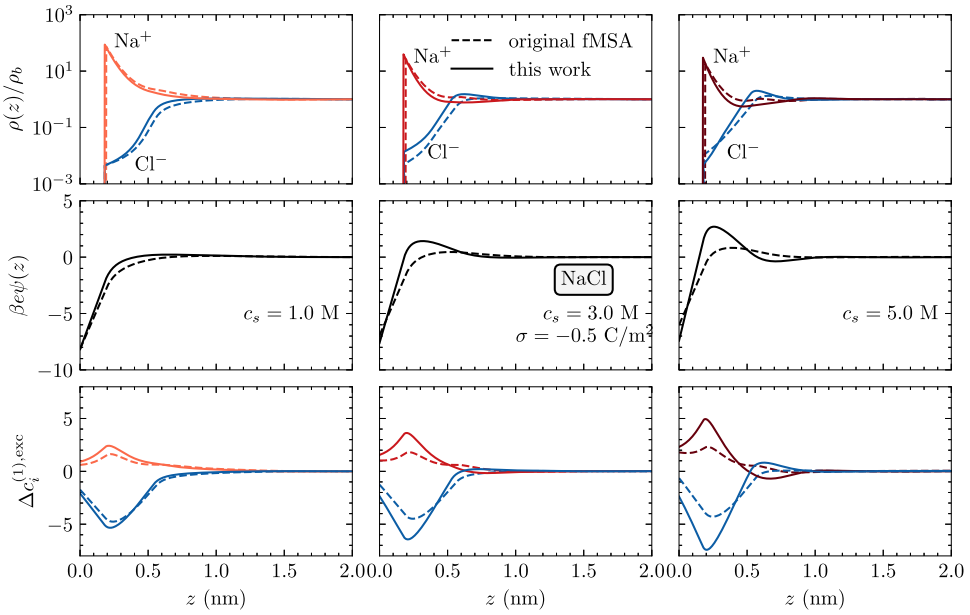

Figure 2. Profiles of each ionic density, the mean electrostatic potential, and the excess first-order direct correlation functions (from top to bottom) of NaCl at three concentrations c_s = 1.0 M (left), 3.0 M (middle), and 5.0 M (right). Dashed Lines: original fMSA results with ionic Pauli diameters and water ϵ_r value. Solid lines: fMSA results with hydrated cation diameter a_+ from fitted parameter as in Table 1 and ϵ_r value from ref 27.

smaller and so is the relative permittivity. These two effects increase the variation of the excess first-order direct correlation functions $\Delta c_i^{(1),\mathrm{exc}}$, as we can see on the lower row of Figure 2.

Figure 3 shows the electrostatic potential values $\psi(z = 0)$ and $\psi(z = a_+/2)$ at the wall position and the diffuse-layer position, respectively, as a function of the wall surface charge density σ for NaCl at salt concentrations of 1.0, 3.0, and 5.0 M. For c_s = 1.0 M, the two cDFT models present the same potential value. But for c_s = 3.0 and 5.0 M, our model presents a higher absolute value of ψ_0 than the original fMSA model for high σ absolute values; e.g., for 5.0 M and σ = −0.5 C/m^2 the wall layer potential values are ψ_0 = −150 mV (fMSA) and ψ_0 = −185 mV (our model). This potential increasing is sharper in the diffuse layer at $z = a_+/2$. For c_s = 3.0 M and σ = −0.5 C/m^2 the diffuse layer potential values are $\psi_{a_+/2}$ = −39 mV (fMSA) and $\psi_{a_+/2}$ = −5 mV (our model). But for c_s = 5.0 M and σ = −0.5 C/m^2, there is a potential value inversion at the diffuse layer with potential values of $\psi_{a_+/2}$ = −16 mV for the original fMSA, and $\psi_{a_+/2}$ = +35 mV for the result in this work. This phenomenon can be explained by the increase in the first-order excess correlation function $c_i^{(1),\mathrm{exc}}$ at the same positions, as presented by the profiles in Figure 2 and previously discussed.

4. CONCLUSIONS

Therefore, in this work we have made a first attempt to describe real electrolyte solutions from the primitive model of the fMSA proposed by Roth and Gillespie.[13] We introduced the cation hard-sphere diameter and electric permittivity corrections necessary to properly describe the thermodynamic quantities of simple electrolyte solutions, e.g., the mean activity coefficient. These corrections turn the cDFT based on fMSA consistent with the MSA equation of state for real ionic solutions. Finally, the fMSA with hydrated cation diameter and electrolyte permittivity predicted a sharp charge inversion on simple salt solutions with a high salt concentration limit near a very highly charged surface. This charge inversion can be

https://doi.org/10.1021/acs.jpcb.2c00816
J. Phys. Chem. B XXXX, XXX, XXX−XXX

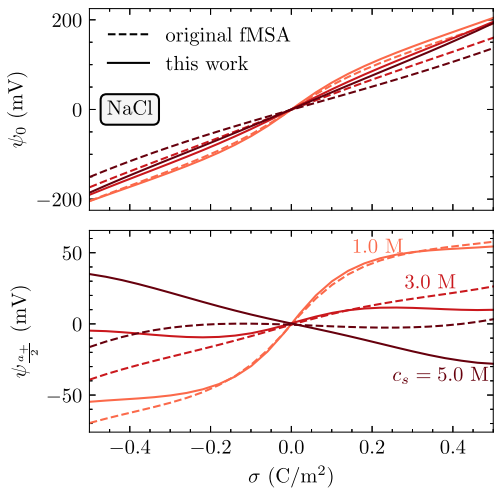

Figure 3. Wall potential ψ_0 (top) and the diffuse-layer potential $\psi_{a_+/2}$ (bottom) as a function of the wall surface charge density σ at two NaCl concentrations. The labels are described in the Figure 2 caption.

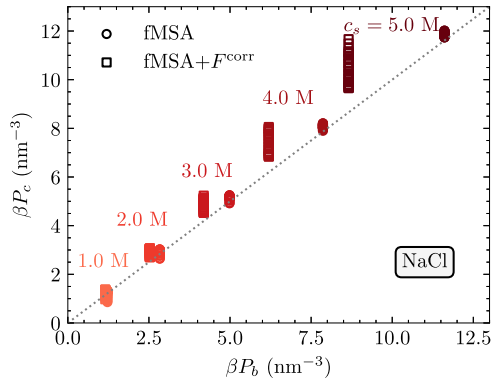

Figure 4. Contact-value theorem calculated using the fMSA with or without our correction functional, F^{corr}.

verified by measurements of the diffuse layer potential inside a simple electrolyte in contact with a charged surface. We emphasize that the cation hydrated diameter and the relative permittivity corrections are inherent to the primitve MSA model to describe real ionic solutions. Therefore, future works in the direction of making these corrections better described by cDFT should be carried out.

APPENDIX

When an electrolyte solution is in contact with a charged surface, it is subject to an electrostatic potential, such that the ionic number density becomes spatially inhomogeneous. The cDFT is the extension of the equation of state to treat inhomogeneous fluids. For this electrolyte solution with temperature T, total volume $\mathcal{V}$, and chemical potential of each species μ_i specified, the grand potential, Ω, is written as

$$\Omega[\{\rho_k(\mathbf{r})\}, \psi(\mathbf{r})] = F^{id} + F^{exc} + F^{coul} + \sum_i \int_{\mathcal{V}} d\mathbf{r}(V_i^{ext}(\mathbf{r}) - \mu_i)\rho_i(\mathbf{r}) + \oint_{\partial\mathcal{V}} d\mathbf{r}\, \sigma(\mathbf{r})\psi(\mathbf{r}) \tag{6}$$

where $\rho_i(\mathbf{r})$ is the local density of the component i, σ is the surface charge density, $\psi(\mathbf{r})$ is the local electrostatic potential, F^{id} is the intrinsic Helmholtz free energy functional of an ideal gas, F^{exc} is the excess Helmholtz free energy functional due to particle−particle interactions, F^{coul} is the free energy due to the presence of the electrostatic potential and the electrostatic interactions between the ions, and V_i^{ext} is the external potential. The volume of the system is $\mathcal{V}$, and $\partial\mathcal{V}$ is the boundary of the system.

The ideal-gas contribution F^{id} is given by the exact expression

$$\beta F^{id}[\{\rho_k(\mathbf{r})\}] = \sum_i \int_{\mathcal{V}} d\mathbf{r}\, \rho_i(\mathbf{r})[\ln(\rho_i(\mathbf{r})\Lambda_i^3) - 1] \tag{7}$$

where $\beta = (k_B T)^{-1}$, k_B is the Boltzmann constant, T is the absolute temperature, and Λ_i is the well-known thermal de Broglie wavelength of ions of species i.

The Coulomb free energy F^{coul} is obtained by the addition of the electric field energy density and the minimal coupling of the interaction between the electrostatic potential $\psi(\mathbf{r})$ and the charge densities $Z_i e\rho_i(\mathbf{r})$. This free energy just considers the electrostatic interactions between the ions at the mean-field level, and it can be written as

$$F^{coul}[\{\rho_k(\mathbf{r})\}, \psi(\mathbf{r})] = -\int_{\mathcal{V}} d\mathbf{r} \frac{\epsilon_0\epsilon_r}{2} |\nabla\psi(\mathbf{r})|^2 + \int_{\mathcal{V}} d\mathbf{r} \sum_i Z_i e\rho_i(\mathbf{r})\psi(\mathbf{r}) \tag{8}$$

where Z_i is the valence of the ion i, e is the elementary charge, ϵ_0 is the vacuum permittivity, and ϵ_r is the relative permittivity.

The Helmholtz free energy functional F^{exc} of the excess contribution can be separated into three terms:

$$F^{exc}[\{\rho_k(\mathbf{r})\}] = F^{hs}[\{\rho_k(\mathbf{r})\}] + F^{ec}[\{\rho_k(\mathbf{r})\}] + F^{corr}[\{\rho_k(\mathbf{r})\}] \tag{9}$$

The term F^{hs} represents the excess Helmholtz free energy functional due to hard-sphere exclusion volume, described by the modified fundamental measure theory (FMT),[29] which provides an accurate description of the hard-sphere fluid structures. In this work, we applied the White-Bear functional[30,31] for the hard-sphere Helmholtz free energy contribution as

$$\beta F^{hs}[\{\rho_k(\mathbf{r})\}] = \int_{\mathcal{V}} d\mathbf{r}\, \Phi_{FMT}(\{n_\alpha(\mathbf{r})\}) \tag{10}$$

where Φ_{FMT} is the local free energy density of a mixture of hard spheres, which is a function of the set of weighted densities, $n_\alpha(\mathbf{r})$. The term F^{ec} in eq 9 represents the excess Helmholtz free energy contribution due to charge distribution correlations, which can be described by the fMSA in the modified form

$$\beta F^{ec}[\{\rho_k(\mathbf{r})\}] = \int_{\mathcal{V}} d\mathbf{r}\, \Phi_{MSA}(\{q_i^{(0)}(\mathbf{r})\}) - \frac{1}{2}\sum_{i,j}\int_{\mathcal{V}} d\mathbf{r} \int_{\mathcal{V}} d\mathbf{r}'\, \Delta\rho_i(\mathbf{r})\Delta c_{ij}^{(2)}(|\mathbf{r} - \mathbf{r}'|)\Delta\rho_j(\mathbf{r}) \tag{11}$$

where Φ_{MSA} is the local free energy density and $q_i^{(0)}(\mathbf{r})$ is the shell-of-charge weighted density of the ith species. The second parcel in eq 11 represents the MSA direct correlation contribution obtained as a generalization of Rosenfeld's method,[32] which expands the MSA functional[15] in a functional Taylor series in powers of the local density difference $\Delta\rho_i(r) = \rho_i(r) - \rho_i^{(b)}$, where $\rho_i^{(b)}$ is the bulk density of the ith species

https://doi.org/10.1021/acs.jpcb.2c00816
J. Phys. Chem. B XXXX, XXX, XXX−XXX

and $\Delta c_{ij}^{(2),\mathrm{MSA}}$ is the second-order direct correlation function from the MSA. It is important to highlight that the modification of the original fMSA proposed here, eq 11, is sufficient to erase the non-MSA chemical potential present in the fMSA but not present in the original MSA. This modification has no effect on the ion density profiles and to the direct correlation functions, but it is essential to describe correctly the thermodynamics quantities, e.g., activity and osmotic coefficients. More details are presented in the Supporting Information.[33] The term F^{corr}, which is not present in the original fMSA, represents the corrections for the real electrolyte solutions chemical potential in a first-order Taylor's expansion approximation on the bulk density as

$$F^{\mathrm{corr}}[\{\rho_k(\mathbf{r})\}] = \sum_i \int_{\mathcal{V}} \mathrm{d}\mathbf{r} \left[\frac{\partial \Phi_{\mathrm{FMT}}^{(b)}}{\partial a_+} \frac{\partial a_+}{\partial \rho_i^{(b)}} + \frac{\partial \Phi_{\mathrm{MSA}}^{(b)}}{\partial a_+} \frac{\partial a_+}{\partial \rho_i^{(b)}} + \frac{\partial \Phi_{\mathrm{MSA}}^{(b)}}{\partial \epsilon_r} \frac{\partial \epsilon_r}{\partial \rho_i^{(b)}} \right] \Delta\rho_i(\mathbf{r}) \tag{12}$$

These corrections are negligible when dealing with ionic solutions where the ions have no hydration effects and the solvents have no salt concentration effects.

The nonelectrostatic external potential is represented by a hard-wall in the form

$$V_i^{\mathrm{ext}}(\mathbf{r}) = \begin{cases} \infty, & \mathbf{r}_\perp < a_i/2 \\ 0, & \text{otherwise} \end{cases} \tag{13}$$

where $\mathbf{r}_\perp$ is the perpendicular distance from the surface to the center of the sphere i and a_i is the hard-sphere diameter of the ith species.

Finally, the last term in eq 6 is the integral representation of the electrostatic potential boundary condition. In fact, the surface charge σ acts as a surface constraint to the electrostatic potential ψ, equivalent to the chemical potential μ_i for the ionic number density ρ_i.

The thermodynamic equilibrium is obtained by extremizing the grand potential Ω, which can be obtained by the functional derivatives as discussed in the Supporting Information.[33] In fact, the equilibrium solution is a saddle point of the grand potential; i.e., it is a minimum with respect to density profile, but it is a maximum with respect to the electric potential.

The equilibrium condition for each charged component is given by

$$\left.\frac{\delta\Omega}{\delta\rho_i(\mathbf{r})}\right|_{\{\mu_k\},\mathcal{V},T} = k_{\mathrm{B}}T \ln[\Lambda_i^3 \rho_i(\mathbf{r})] + \frac{\delta F^{\mathrm{exc}}}{\delta\rho_i(\mathbf{r})} + Z_i e\psi(\mathbf{r}) + V_i^{\mathrm{ext}}(\mathbf{r}) - \mu_i = 0 \tag{14}$$

and for the electrostatic potential it is

$$\left.\frac{\delta\Omega}{\delta\psi(\mathbf{r})}\right|_{\{\mu_k\},\mathcal{V},T} = \epsilon_0\epsilon_r\nabla^2\psi(\mathbf{r}) + \sum_i Z_i e\rho_i(\mathbf{r}) = 0 \tag{15}$$

valid in the whole volume $\mathcal{V}$, and its boundary condition is

$$\left.\frac{\delta\Omega}{\delta\psi(\mathbf{r})}\right|_{\{\mu_k\},\mathcal{V},T} = \epsilon_0\epsilon_r\hat{\mathbf{n}}(\mathbf{r})\cdot\nabla\psi(\mathbf{r}) + \sigma(\mathbf{r}) = 0 \tag{16}$$

valid on the boundary surface $\partial\mathcal{V}$, where $\hat{\mathbf{n}}(\mathbf{r})$ is denoting the vector normal to the surface pointing inward to the system. Equation 15 is the well-known Poisson's equation[34,35] of the electrostatic potential with the boundary conditions from eq 16. Moreover, eq 14 reduces to the solution of a modified PB equation where the distribution of each ion density is determined by

$$\rho_i(\mathbf{r}) = \rho_i^{(b)} \mathrm{e}^{-\beta Z_i e\psi(\mathbf{r}) - \beta V_i^{\mathrm{ext}}(\mathbf{r}) + \Delta c_i^{(1),\mathrm{exc}}(\mathbf{r})} \tag{17}$$

where $\Delta c_i^{(1),\mathrm{exc}}(\mathbf{r}) = c_i^{(1),\mathrm{exc}}(\mathbf{r}) + \beta\mu_i^{\mathrm{exc}}$ is the variation of the first-order excess correlation function.

With the introduction of the hard-sphere cation diameter and the electric permittivity corrections, the first-order excess correlation functions $c_i^{(1),\mathrm{exc}}(\mathbf{r})$ are the sum of the following contributions

$$c_i^{(1),\mathrm{hs}}(\mathbf{r}) \equiv -\beta\frac{\delta F^{\mathrm{hs}}}{\delta\rho_i(\mathbf{r})} = -\int_{\mathcal{V}} \mathrm{d}\mathbf{r}' \sum_\alpha \frac{\partial \Phi_{\mathrm{FMT}}}{\partial n_\alpha(\mathbf{r}')} \omega_i^{(\alpha)}(\mathbf{r} - \mathbf{r}') \tag{18}$$

$$c_i^{(1),\mathrm{ec}}(\mathbf{r}) \equiv -\beta\frac{\delta F^{\mathrm{ec}}}{\delta\rho_i(\mathbf{r})} = -\int_{\mathcal{V}} \mathrm{d}\mathbf{r}' \frac{\delta \Phi_{\mathrm{MSA}}}{\delta q_i^{(0)}(\mathbf{r}')} \omega_i^{(s)}(\mathbf{r} - \mathbf{r}') - \sum_j \int_{\mathcal{V}} \mathrm{d}\mathbf{r}'\, \Delta c_{ij}^{(2),\mathrm{MSA}}(|\mathbf{r} - \mathbf{r}'|)\Delta\rho_j(\mathbf{r}) \tag{19}$$

and

$$c_i^{(1),\mathrm{corr}}(\mathbf{r}) \equiv -\beta\frac{\delta F^{\mathrm{corr}}}{\delta\rho_i(\mathbf{r})} = -\frac{\partial \Phi_{\mathrm{FMT}}^{(b)}}{\partial a_+}\frac{\partial a_+}{\partial \rho_i^{(b)}} - \frac{\partial \Phi_{\mathrm{MSA}}^{(b)}}{\partial \epsilon_r}\frac{\partial \epsilon_r}{\partial \rho_i^{(b)}} - \frac{\partial \Phi_{\mathrm{MSA}}^{(b)}}{\partial a+}\frac{\partial a+}{\partial \rho_i^{(b)}} \tag{20}$$

where $\omega_i^{(\alpha)}(r)$ are the weight functions from FMT, $\omega_i^{(s)}(r)$ are the weight functions from fMSA, and $b_i = a_i + 1/\Gamma_b$ is the shell diameter of the ith species, i.e., the diameter of the ion plus the inverse of the MSA screening parameter. The terms from eq 20 were generated to correct the bulk values of the first-order correlation functions which correspond to the excess chemical potential values, i.e., $c_i^{(1),\mathrm{exc}}(\mathbf{r}) \to -\beta\mu_i^{\mathrm{exc}}$ when $\rho_i(\mathbf{r}) \to \rho_i^{(b)}$. The excess chemical potential is now $\mu_i^{\mathrm{exc}} = \mu_i^{\mathrm{hs}} + \mu_i^{\mathrm{ec}} + \mu_i^{\mathrm{corr}}$, and it can be written in terms of the free energy densities Φ_{FMT} and Φ_{MSA} calculated in the bulk conditions as follows:

$$\beta\mu_i^{\mathrm{hs}} = \frac{\partial \Phi_{\mathrm{FMT}}^{(b)}}{\partial \rho_i^{(b)}}, \qquad \beta\mu_i^{\mathrm{ec}} = \frac{\partial \Phi_{\mathrm{MSA}}^{(b)}}{\partial \rho_i^{(b)}} \tag{21}$$

and

$$\beta\mu_i^{\mathrm{corr}} = \frac{\partial \Phi_{\mathrm{FMT}}^{(b)}}{\partial a_+}\frac{\partial a_+}{\partial \rho_i^{(b)}} + \frac{\partial \Phi_{\mathrm{MSA}}^{(b)}}{\partial \epsilon_r}\frac{\partial \epsilon_r}{\partial \rho_i^{(b)}} + \frac{\Phi_{\mathrm{MSA}}^{(b)}}{\partial a_+}\frac{\partial a_+}{\partial \rho_i^{(b)}} \tag{22}$$

The inclusion of the F^{corr} from eq 12 does not affect the density profile as well. In fact, the variation of the first-order correlation function $\Delta c_i^{(1),\mathrm{corr}}(\mathbf{r}) = c_i^{(1),\mathrm{corr}}(\mathbf{r}) + \beta\mu_i^{\mathrm{corr}}$ is null through the system, and it does not add any modification on the ionic density profiles. The results of Figures 2 and 3 were generated with just the fMSA, i.e., without the F^{corr}.

One of the great tests of thermodynamic consistency of cDFT is the contact-value theorem. For ions of species i in contact with a charged wall, the contact-value theorem[36,37] requires that the pressure of the bulk fluid, P_b, far from the surface be determined by

https://doi.org/10.1021/acs.jpcb.2c00816
J. Phys. Chem. B XXXX, XXX, XXX−XXX

$$P_b = k_B T \sum_i \rho_i(a_i/2) - \frac{\sigma^2}{2\epsilon_0\epsilon_r} \quad (23)$$

where $\rho_i(a_i/2)$ are ionic densities at the surface and σ the surface charge density. The bulk pressure can be obtained by the grand potential in the form $P_b = -\Omega_b/V$.

Figure 4 compares the cDFT predictions for the reduced bulk osmotic pressure versus the reduced contact pressure, as presented by the eq 23. The original fMSA has a great performance when compared to our proposed functional. We expect the deviations of our model from the contact-value theorem because they are associated with the bulk density expansion of the free energy functional. In fact, similar deviations from the contact theorem are present in the BFD formulation.[38] These results demonstrate that it is necessary to go beyond the Taylor's expansion in the formulation of the correction functional, F^{corr}. However, there is a huge difficulty in treating the derivative terms with respect to the diameter of the cation because all weight functions depend on the diameter and must be derived as well.

■ ASSOCIATED CONTENT

Supporting Information

The Supporting Information is available free of charge at https://pubs.acs.org/doi/10.1021/acs.jpcb.2c00816.

All the functional derivatives of Ω and the numerical implementations (PDF)

■ AUTHOR INFORMATION

Corresponding Authors

Elvis do A. Soares − *Engenharia de Processos Químicos e Bioquímicos (EPQB), Escola de Química, Universidade Federal do Rio de Janeiro, Rio de Janeiro, RJ 21941-909, Brazil;* orcid.org/0000-0002-6202-9875; Email: elvis.asoares@gmail.com

Frederico W. Tavares − *Engenharia de Processos Químicos e Bioquímicos (EPQB), Escola de Química, Universidade Federal do Rio de Janeiro, Rio de Janeiro, RJ 21941-909, Brazil; Programa de Engenharia Química, COPPE, Universidade Federal do Rio de Janeiro, Rio de Janeiro, RJ 21941-909, Brazil;* orcid.org/0000-0001-8108-1719; Email: tavares@eq ufrj.br

Authors

Nathalia S. Vernin − *Departamento de Engenharia Sanitária e do Meio Ambiente, Faculdade de Engenharia, Universidade do Estado do Rio de Janeiro, Rio de Janeiro, RJ 20550-900, Brazil;* orcid.org/0000-0002-3705-4884

Mirella S. Santos − *Laboratoire de Chimie, École Normale Supérieure de Lyon, Lyon 69007, France;* orcid.org/0000-0002-9590-5536

Complete contact information is available at: https://pubs.acs.org/10.1021/acs.jpcb.2c00816

Notes

The authors declare no competing financial interest.

■ ACKNOWLEDGMENTS

The authors thank the financial support from the Brazilian National Agency of Petroleum, Natural Gas and Biofuels (ANP, Brazil), and PETROBRAS through the Clause of Investments in Research, Development, and Innovation. This study was also partially financed by the National Council for Technological and Scientific Development (CNPq, Brazil), the Coordination for the Improvement of Higher Education Personnel (CAPES, Brazil), and Carlos Chagas Filho Research Support Foundation (FAPERJ, Brazil).

■ REFERENCES

(1) Grosberg, A. Y.; Nguyen, T. T.; Shklovskii, B. I. Colloquium: The physics of charge inversion in chemical and biological systems. *Rev. Mod. Phys.* **2002**, *74*, 329−345.

(2) Diehl, A.; Levin, Y. Colloidal charge reversal: Dependence on the ionic size and the electrolyte concentration. *J. Chem. Phys.* **2008**, *129*, 124506.

(3) Levin, Y. When do like charges attract? *Physica A: Statistical Mechanics and its Applications* **1999**, *265*, 432−439.

(4) dos Santos, A. P.; Levin, Y. Like-Charge Attraction between Metal Nanoparticles in a 1:1 Electrolyte Solution. *Phys. Rev. Lett.* **2019**, *122*, 248005.

(5) Cats, P.; Evans, R.; Härtel, A.; van Roij, R. Primitive model electrolytes in the near and far field: Decay lengths from DFT and simulations. *J. Chem. Phys.* **2021**, *154*, 124504.

(6) Kaja, M.; Silvestre-Alcantara, W.; Lamperski, S.; Henderson, D.; Bhuiyan, L. B. Monte Carlo investigation of structure of an electric double layer formed by a valency asymmetric mixture of charged dimers and charged hard spheres. *Mol. Phys.* **2015**, *113*, 1043−1052.

(7) Voukadinova, A.; Valiskó, M.; Gillespie, D. Assessing the accuracy of three classical density functional theories of the electrical double layer. *Phys. Rev. E* **2018**, *98*, 1−15.

(8) Yu, Y.-X.; Wu, J.; Gao, G.-H. Density-functional theory of spherical electric double layers and ζ potentials of colloidal particles in restricted-primitive-model electrolyte solutions. *J. Chem. Phys.* **2004**, *120*, 7223−7233.

(9) Wang, Z.; Liu, L.; Neretnieks, I. The weighted correlation approach for density functional theory: A study on the structure of the electric double layer. *J. Phys.: Condens. Matter* **2011**, *23*, 175002.

(10) Mier-y-Teran, L.; Suh, S. H.; White, H. S.; Davis, H. T. A nonlocal free-energy density-functional approximation for the electrical double layer. *J. Chem. Phys.* **1990**, *92*, 5087−5098.

(11) Kierlik, E.; Rosinberg, M. L. Density-functional theory for inhomogeneous fluids: Adsorption of binary mixtures. *Phys. Rev. A* **1991**, *44*, 5025−5037.

(12) Rosenfeld, Y. Free energy model for inhomogeneous fluid mixtures: Yukawa-charged hard spheres, general interactions, and plasmas. *J. Chem. Phys.* **1993**, *98*, 8126−8148.

(13) Roth, R.; Gillespie, D. Shells of charge: A density functional theory for charged hard spheres. *J. Phys.: Condens. Matter* **2016**, *28*, 244006.

(14) Gillespie, D.; Nonner, W.; Eisenberg, R. S. Coupling Poisson Nernst Planck and density functional theory to calculate ion flux. *J. Phys.: Condens. Matter* **2002**, *14*, 12129−12145.

(15) Gillespie, D.; Nonner, W.; Eisenberg, R. S. Density functional theory of charged, hard-sphere fluids. *Phys. Rev. E* **2003**, *68*, 031503.

(16) Jiang, J.; Gillespie, D. Revisiting the Charged Shell Model: A Density Functional Theory for Electrolytes. *J. Chem. Theory Comput.* **2021**, *17*, 2409−2416.

(17) Blum, L. Mean spherical model for asymmetric electrolytes I. Method of solution. *Mol. Phys.* **1975**, *30*, 1529−1535.

(18) Blum, L.; Hoeye, J. S. Mean spherical model for asymmetric electrolytes. 2. Thermodynamic properties and the pair correlation function. *J. Phys. Chem.* **1977**, *81*, 1311−1316.

(19) Simonin, J.-P.; Bernard, O.; Blum, L. Ionic Solutions in the Binding Mean Spherical Approximation: Thermodynamic Properties of Mixtures of Associating Electrolytes. *J. Phys. Chem. B* **1999**, *103*, 699−704.

(20) Kontogeorgis, G. M.; Folas, G. K. *Thermodynamic Models for Industrial Applications: From Classical and Advanced Mixing Rules to Association Theories*; John Wiley & Sons: 2009.

(21) Triolo, R.; Grigera, J. R.; Blum, L. Simple electrolytes in the mean spherical approximation. *J. Phys. Chem.* **1976**, *80*, 1858−1861.
(22) Triolo, R.; Blum, L.; Floriano, M. A. Simple electrolytes in the mean spherical approximation. 2. Study of a refined model. *J. Phys. Chem.* **1978**, *82*, 1368−1370.
(23) Simonin, J.-P.; Blum, L.; Turq, P. Real Ionic Solutions in the Mean Spherical Approximation. 1. Simple Salts in the Primitive Model. *J. Phys. Chem.* **1996**, *100*, 7704−7709.
(24) Simonin, J.-P. Real Ionic Solutions in the Mean Spherical Approximation. 2. Pure Strong Electrolytes up to Very High Concentrations, and Mixtures, in the Primitive Model. *J. Phys. Chem. B* **1997**, *101*, 4313−4320.
(25) Robinson, R. A.; Stokes, R. H. *Electrolyte Solutions*, 2nd ed.; Dover: 2002.
(26) Liu, Y.; Li, Z.; Mi, J.; Zhong, C. Modeling of Aqueous Electrolyte Solutions Based on Primitive and First-Order Mean Spherical Approximation. *Ind. Eng. Chem. Res.* **2008**, *47*, 1695−1701.
(27) Zuber, A.; Cardozo-Filho, L.; Cabral, V. F.; Checoni, R. F.; Castier, M. An empirical equation for the dielectric constant in aqueous and nonaqueous electrolyte mixtures. *Fluid Phase Equilib.* **2014**, *376*, 116−123.
(28) Hamer, W. J.; Wu, Y. Osmotic Coefficients and Mean Activity Coefficients of Uni-univalent Electrolytes in Water at 25°C. *J. Phys. Chem. Ref. Data* **1972**, *1*, 1047−1100.
(29) Rosenfeld, Y. Free-energy model for the inhomogeneous hard-sphere fluid mixture and density-functional theory of freezing. *Phys. Rev. Lett.* **1989**, *63*, 980−983.
(30) Yu, Y. X.; Wu, J. Structures of hard-sphere fluids from a modified fundamental-measure theory. *J. Chem. Phys.* **2002**, *117*, 10156−10164.
(31) Roth, R.; Evans, R.; Lang, A.; Kahl, G. Fundamental measure theory for hard-sphere mixtures revisited: The white bear version. *J. Phys.: Condens. Matter* **2002**, *14*, 12063−12078.
(32) Rosenfeld, Y. Free energy model for inhomogeneous fluid mixtures: Yukawa-charged hard spheres, general interactions, and plasmas. *J. Chem. Phys.* **1993**, *98*, 8126−8148.
(33) Real Ionic Solutions in the Functionalized Mean Spherical Approximation. Supplementary Material, 2021.
(34) Landau, L. D.; Pitaevskii, L. P.; Lifshitz, E. M. *Electrodynamics of Continuous Media*, 2nd ed.; Course of Theoretical Physics; Butterworth-Heinemann: 1984; Vol. *8*.
(35) Jackson, J. D. *Classical Electrodynamics*, 3rd ed.; Wiley: 1998.
(36) Hansen, J.-P.; McDonald, I. R. *Theory of Simple Liquids: With Applications to Soft Matter*; Academic Press: 2013.
(37) Israelachvili, J. N. *Intermolecular and Surface Forces*; Academic Press: 2015.
(38) Jiang, J.; Cao, D.; Henderson, D.; Wu, J. A contact-corrected density functional theory for electrolytes at an interface. *Phys. Chem. Chem. Phys.* **2014**, *16*, 3934.

https://doi.org/10.1021/acs.jpcb.2c00816
J. Phys. Chem. B XXXX, XXX, XXX−XXX